International Journal of Pure and Applied Mathematics

Volume 36 No. 4 2007, 393-405

THE MICROPOLAR FLUID MODEL FOR BLOOD FLOW THROUGH A STENOTIC ARTERIES

Kh.S. Mekheimer[1], M.A. El Kot[2 §]

[1]Department of Mathematics
Faculty of Science
Al-Azhar University
Nasr City, Cairo, 11884, EGYPT
e-mail: kh_mekheimer@yahoo.com

[2]Department of Mathematics
Faculty of Education
Suez Canal University
Suez, EGYPT
e-mail: m_aaosman@yahoo.com

Abstract: A micropolar model for blood flow through a horizontally non-symmetreic artery with a mild stenosis is presented. To estimate the effect of the stenosis shape, a suitable geometry has been considered such that the (x-axis) shape of the stenosis can be changed easily just by varying a parameter (referred to as the shape parameter). Flow parameters such as velocity, the resistance to flow (the resistance impedance), the wall shear stress distribution in the stenotic region and its magnitude at the maximum height of the stenosis (stenosis throat) have been computed for different shape parameter n, the coupling number N and the micropolar parameter m. It is shown that the resistance to flow decreases with increasing values of the parameter determining the stenosis shape n also the resistance to flow increases with the coupling parameter N and decreases with the micropolar parameter m. The magnitudes of the resistance to flow are higher in the case of a micropolar fluid model than in the case of a Newtonian fluid model. The wall shear stress and the shearing stress on the wall at the maximum height of the stenosis possess an inverse variation to the resistance to flow with respect to N and m. Finally, the effect of the

Received: January 27, 2007

§Correspondence author

coupling stress parameters N and m on the horizontal velocity is discussed.

AMS Subject Classification: 92C50, 92C45
Key Words: micropolar model, blood flow, horizontally nonsymmetreic artery, stenosis

1. Introduction

One of the leading causes of the deaths in the world is due to heart diseases, and the most commonly heard names among the same are ischemia, atherosclerosis and angina pectoris. Ischemia is the deficiency of the oxygen in apart of the body, usually temporary. It can due to a constriction (stenosis) or obstruction in the blood vessel supplying that part. Atherosclerosis is a type of arteriosclerosis. It comes from the Greek words athero (meaning gruel or paste) and sclerosis (hardness), it involves deposits of fatty substances, cholesterol, cellular waste products, calcium and fibrin (clothing material in the blood) in the inner lining of an artery. The build up that results is called plaque. Plaque may partially or totally block the blood flow through an artery.

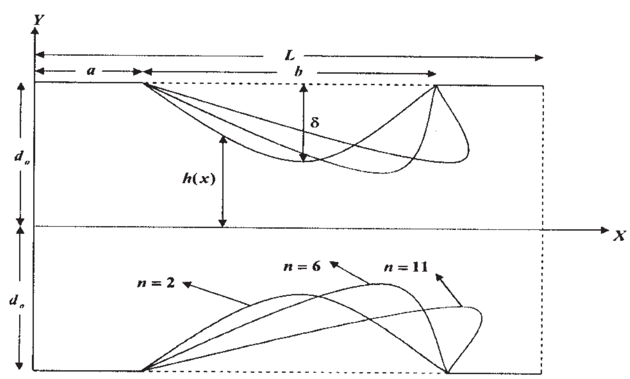

Figure 1: Geometry of the stenosed chanal

The theory of micropolar fluid due to Eringen [3] is a subclass of microfluids. The micropolar fluid, e.g., liquid crystals, suspensions and animal blood, etc., consists of randomly oriented bar-like elements or dumbbell molecules and each volume element has microrotation about its centroid, in addition to translatory motion in an average sense. The model of micropolar fluid introduced by Eringen [3] represents fluid consisting of rigid, randomly oriented (or spherical) particles suspended in viscous medium where the deformation of the particles

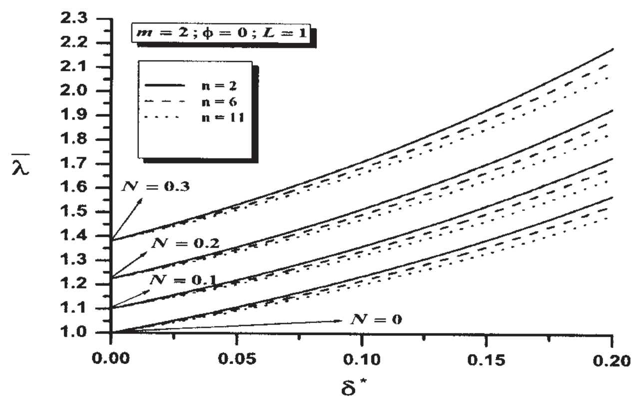

Figure 2: Variation of dimensional resistance of flow, $\bar{\lambda}$, with δ^* for different values of N and n

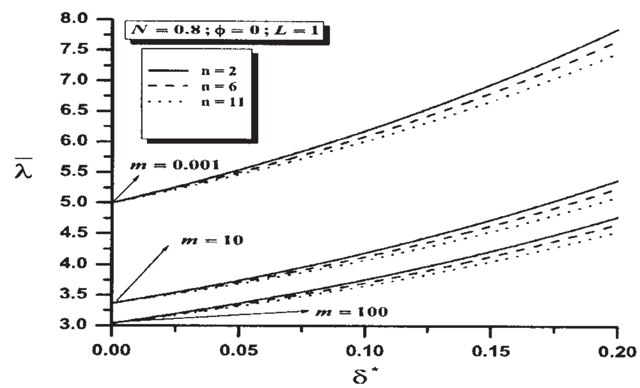

Figure 3: Variation of dimensional resistance of flow, $\bar{\lambda}$, with δ^* for different values of m and n

is ignored, micropolar fluids exhibit some micromotion of the fluid elements. Further, they can sustain couple stress. The micropolar fluid is considered to the model of the blood flow in small arteries and the calculation of theoretical velocity profiles is observed in good agreement with experimental data.

A number of researchers have studied the flow of blood through stenosed arteries [2-9]. In the paper, we study the blood flow through a horizontally nonsymmetric artery with a mild stenosis, when blood is represented by a micropolar fluid, the effects of resistance to flow, the wall shear stress distribution in the stenotic region and its magnitude at the maximum height of the stenosis are discussed numerically and explained graphically.

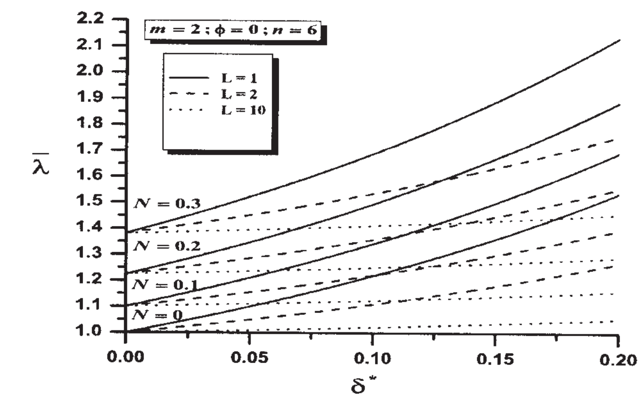

Figure 4: Variation of dimensional resistance of flow, $\bar{\lambda}$, with δ^* for different values of N and L

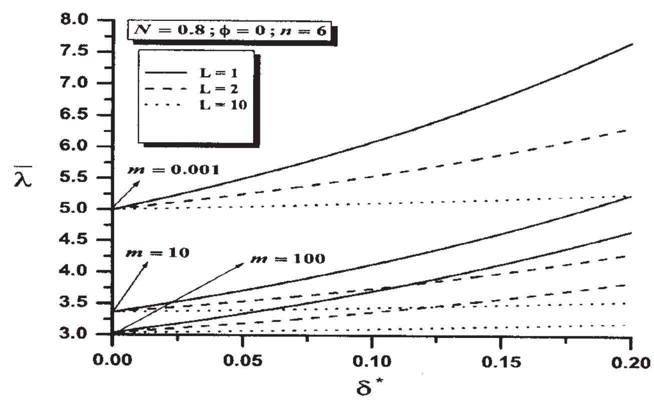

Figure 5: Variation of dimensional resistance of flow, $\bar{\lambda}$, with δ^* for different values of m and L

2. Formulation of the Problem

Consider a channel of width $2d_o$ and length L bounded by two walls. Let X and Y axes be chosen along and perpendicular to the walls respectively; u and v be the longitudinal and transverse velocities respectively. The geometry of the stenosis which is assumed to be vertically symmetric can be described as

$$h(x) = \begin{cases} d_o[1 - \eta(b^{n-1}(x-a) - (x-a)^n)]\,, & a \le x \le a+b\,, \\ d_o\,, & \text{otherwise}\,. \end{cases} \tag{1}$$

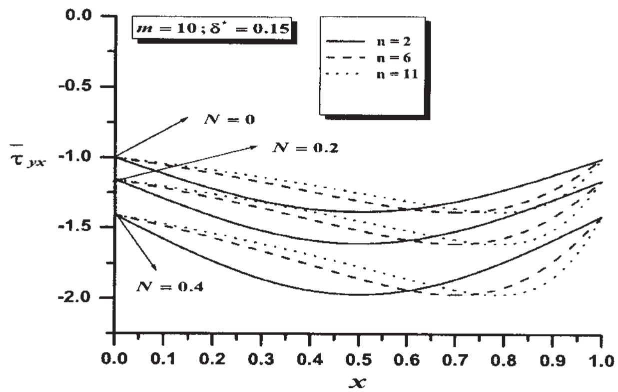

Figure 6: Dimensionless wall shear, $\bar{\tau}_{yx}$, distributions in the stenotic region for different values of N and n

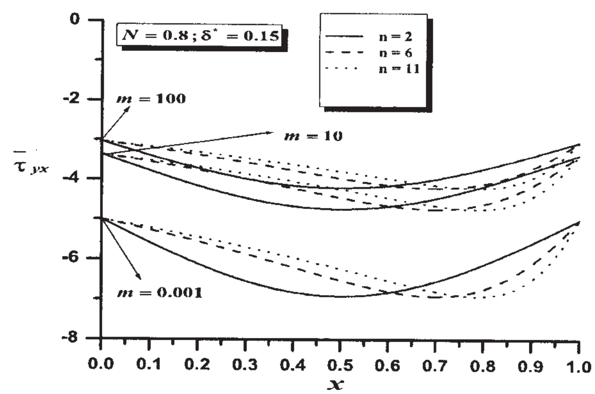

Figure 7: Dimensionless wall shear, $\bar{\tau}_{yx}$, distributions in the stenotic region for different values of m and n

Here $h(x)$ and d_o are the width of the channel with and without stenosis, respectively. b is the length of the stenosis, $n(\geq 2)$ is a parameter determining the shape of the constriction profile and referred to as the shape parameter (the symmetric stenosis occurs for $n = 2$) and a indicates its location (as shown in Figure 1). The parameter η is given by

$$\eta = \frac{\delta}{d_o b^n} \frac{n^{n/(n-1)}}{(n-1)}, \qquad (2)$$

where δ denotes the maximum height of the stenosis located at $x = a + \frac{b}{n^{1/(n-1)}}$.

For this flow let the velocity vector is given by $\mathbf{V} = \{u, v, 0\}$ and the micro-

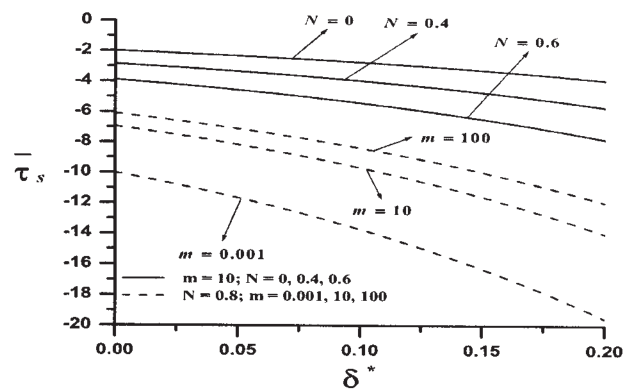

Figure 8: Variation of dimensionless resistance to flow, $\bar{\lambda}$, with N for different values of Δ^*

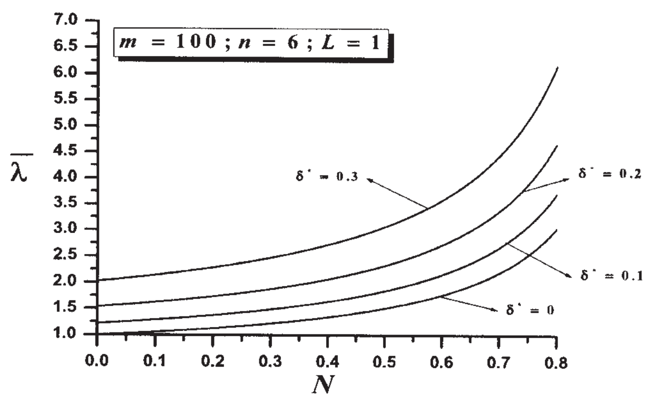

Figure 9: Variation of dimensionless resistance to flow, $\bar{\lambda}$, with m for different values of Δ^*

rotation vector $\mathbf{w} = \{0, 0, \nu\}$. The governing equations of steady laminar flow of an incompressible micropolar fluid can be written as:

$$\frac{\partial u}{\partial x} + \frac{\partial v}{\partial y} = 0, \tag{3}$$

$$\rho(u\frac{\partial u}{\partial x} + v\frac{\partial u}{\partial y}) = -\frac{\partial p}{\partial x} + (\mu + \kappa)(\frac{\partial^2 u}{\partial x^2} + \frac{\partial^2 u}{\partial y^2}) + \kappa\frac{\partial \nu}{\partial y}, \tag{4}$$

$$\rho(u\frac{\partial v}{\partial x} + v\frac{\partial v}{\partial y}) = -\frac{\partial p}{\partial y} + (\mu + \kappa)(\frac{\partial^2 v}{\partial x^2} + \frac{\partial^2 v}{\partial y^2}) - \kappa\frac{\partial \nu}{\partial x}, \tag{5}$$

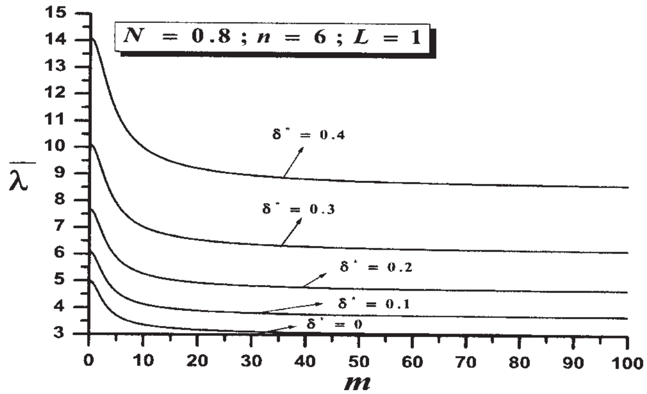

Figure 10: Variation of velocity u with y for different values of N

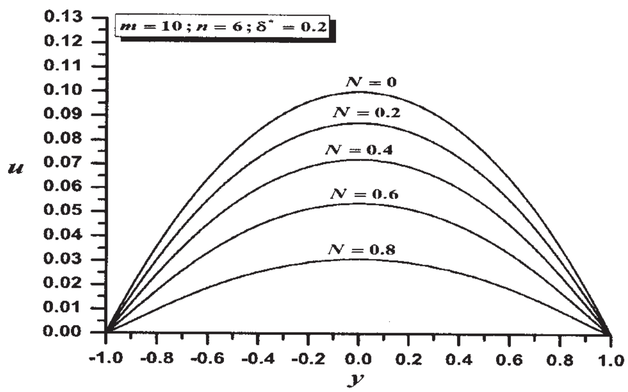

Figure 11: Variation of velocity u with y for different values of m

$$\rho j(u\frac{\partial \nu}{\partial x} + v\frac{\partial \nu}{\partial y}) = -2\kappa\nu - \kappa(\frac{\partial v}{\partial x} - \frac{\partial u}{\partial y}) + \gamma(\frac{\partial^2 \nu}{\partial x^2} + \frac{\partial^2 \nu}{\partial y^2}). \tag{6}$$

The boundary conditions are

$$u = 0, \qquad \nu = 0 \qquad \text{at} \qquad y = \pm h(x), \tag{7}$$

where the material constants μ, κ and γ satisfy the following inequalities (see [9])

$$2\mu + \kappa \geq 0, \qquad \kappa \geq 0, \qquad \gamma > 0. \tag{8}$$

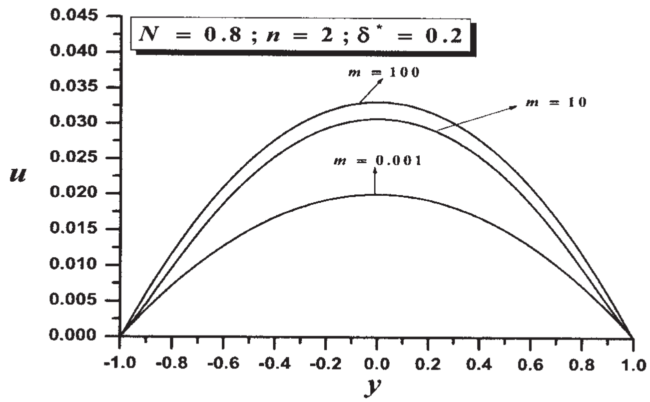

Figure 12:

Introducing the following nondimensional variables

$$x' = \frac{x}{b}, \quad r' = \frac{r}{d_0}, \quad u' = \frac{u}{u_0}, \quad v' = \frac{bv}{u_0\delta}, \\ h' = \frac{h}{d_0}, \quad p' = \frac{d_0^2 p}{u_0 b\mu}, \quad j' = \frac{j}{d_0^2}, \quad \nu = \frac{d_0\nu}{u_0}, \tag{9}$$

into equations (3)-(6) and dropping the dashes. The appropriate equations describing the steady flow of a micropolar fluid in the case of a mild stenosis $(\frac{\delta}{d_0} \ll 1)$, subject to the additional conditions [10], [8], [7], [11]

$$(i) \qquad R_e \frac{\delta n^{\frac{1}{n-1}}}{b} \ll 1\,, \tag{10}$$

$$(ii) \qquad \frac{d_0 n^{\frac{1}{n-1}}}{b} \sim O(1)\,, \tag{11}$$

may be written as

$$\frac{\partial p}{\partial x} = \frac{1}{1-N}\{\frac{\partial^2 u}{\partial y^2} + N\frac{\partial \nu}{\partial y}\}, \tag{12}$$

$$\frac{\partial p}{\partial y} = 0, \tag{13}$$

$$2\nu = -\frac{\partial u}{\partial y} + \frac{2-N}{m^2}\frac{\partial^2 \nu}{\partial y^2}, \tag{14}$$

where u_0 is the velocity averaged over the section of the channel of width d_0, $R_e = \frac{\rho u_o d_o}{\mu}$ is the Reynolds number, $N = \frac{k}{(\mu+k)}$ is the coupling number $(0 \leq N \prec 1)$ [9] and $m^2 = \frac{d_0^2 k(2\mu+k)}{\gamma(\mu+k)}$ is the micropolar parameter.

The corresponding boundary conditions are

$$u = 0, \qquad \nu = 0 \qquad \text{at} \qquad y = \pm h(x),$$

where

$$h(x) = 1 - \eta * ((x-\phi) - (x-\phi)^n), \qquad \phi \leq x \leq \phi + 1 \tag{15}$$

and

$$\eta * = \frac{\delta^* n^{n/(n-1)}}{(n-1)}, \quad \delta^* = \frac{\delta}{d_0}, \quad \phi = \frac{a}{b}. \tag{16}$$

Noting the fact p is a function of x only from equation (13), equation (12) is rewritten in the form

$$\frac{\partial}{\partial y}\{\frac{\partial u}{\partial y} + N\nu\} = (1-N)\frac{\partial p}{\partial x}, \tag{17}$$

hence, we get

$$\frac{\partial u}{\partial y} = (1-N)\frac{\partial p}{\partial x}y + A - N\nu. \tag{18}$$

Using equation (18) in equation (14), we get

$$\frac{\partial^2 \nu}{\partial y^2} - m^2\nu = \frac{(1-N)m^2}{(2-N)}\{\frac{r}{2}\frac{\partial p}{\partial x}y + \frac{A}{(1-N)}\}, \tag{19}$$

and its general solution is

$$\nu(x,y) = B\cosh(my) + C\sinh(my) - \frac{(1-N)}{(2-N)}\{\frac{r}{2}\frac{\partial p}{\partial x}y + \frac{A}{(1-N)}\}. \tag{20}$$

Substituting equation (20) into equation (18) and integrating we obtain

$$u(x,y) = (\frac{1-N}{2-N})\frac{\partial p}{\partial x}y^2 + (\frac{2A}{2-N})y - \frac{N}{m}(B\sinh(my) + c\cosh(my)) + D, \tag{21}$$

where $A(x), B(x), C(x)$ and $D(x)$ are the constants of integration, by using the boundary conditions, we get

$$u(x,y) = (\frac{1-N}{2-N})(\frac{-\partial p}{\partial x})\{h^2 - y^2$$

$$+\frac{Nh}{m\sinh(mh)}(\cosh(my)-\cosh(mh))\}, \quad (22)$$

$$\nu(x,y)=(\frac{1-N}{2-N})(\frac{\partial p}{\partial x})\{\frac{h\sinh(my)}{\sinh(mh)}-y\}. \quad (23)$$

We can find the volume rate $Q(x)$ by

$$Q(x)=\int_0^h u(x,y)dy=\frac{-1}{3}\frac{\partial p}{\partial x}\frac{1}{F(x)}, \quad (24)$$

where

$$F(x)=\frac{(2-N)m^2\sinh(mh)}{2m^2(1-N)h^3\sinh(mh)-3N(1-N)h(hm\cosh(mh)-\sinh(mh))}. \quad (25)$$

The pressure drop Δp ($=p$ at $x=0$, $-p$ at $x=L$) across the stenosis between the sections $x=0$ and $x=L$ is obtained from equation (24) as

$$\Delta p=\int_0^L(\frac{-dp}{dx})dx=3Q\int_0^L F(x)dx. \quad (26)$$

3. The Resistance Impedance

The resistance to flow (resistance impedance) is obtained from equation (26) as

$$\lambda=\frac{\Delta p}{Q}=3\{\int_0^a F(x)|_{h=1}dx+\int_a^{a+b}F(x)dx+\int_{a+b}^L F(x)|_{h=1}dx\}. \quad (27)$$

4. The Expression for the Wall Shear Stress

The nonzero shear stress in our problem are given by

$$\tau_{xy}=\mu\frac{\partial u}{\partial y}-k\nu, \qquad \tau_{yx}=(\mu+\kappa)\frac{\partial u}{\partial y}+\kappa\nu. \quad (28)$$

By using the equation (9) and let $\tau'=\frac{d_o\tau}{\mu u_o}$ we can find the dimensionalless nonzero shear stresses by

$$\tau_{xy}=\frac{\partial u}{\partial y}-(\frac{N}{1-N})\nu, \quad (29)$$

$$\tau_{yx} = \frac{1}{1-N}(\frac{\partial u}{\partial y} + N\nu). \tag{30}$$

From equation (30) we can find the expression for the wall shear stress by

$$\tau_{yx} = \frac{1}{(1-N)}\frac{\partial u}{\partial y}|_{y=h}, \tag{31}$$

where $\nu = 0$ at $y = h$, by using equation (21) we can find

$$\tau_{yx} = -3Qh(x)F(x). \tag{32}$$

We can note that the shearing stress at the stenosis throat (i.e the wall shear at the maximum height of the stenosis located at $x = \frac{a}{b} + \frac{1}{n^{1/(n-1)}}$, i.e. $\tau_s = \tau_{yx}|_{h=1-\delta^*}$)

$$\tau_s = -3Q(1-\delta^*)F(x)|_{h=(1-\delta^*)}. \tag{33}$$

We can find the final expressions for the dimensionless resistance to $\bar{\lambda}$, the wall shear stress $\bar{\tau}_{yx}$ and the shearing stress at the throat $\bar{\tau}_s$ by

$$\bar{\lambda} = (1 - \frac{b}{L})I + \frac{1}{L}\int_a^{a+b} F(x)dx, \tag{34}$$

$$\bar{\tau}_{yx} = -h(x)F(x), \tag{35}$$

$$\bar{\tau}_s = -(1-\delta^*)F(x)|_{h=(1-\delta^*)}, \tag{36}$$

where

$$\bar{\lambda} = \frac{\lambda}{\lambda_0}, \quad \bar{\tau}_{rx} = \frac{\tau_{rx}}{\tau_0}, \quad \bar{\tau}_s = \frac{\tau_s}{\tau_0}, \quad \lambda_0 = 3L, \quad \tau_0 = 3Q, \tag{37}$$

and λ_0, τ_0 are the resistance to flow and the wall shear stress for a flow in a normal artery (no stenosis).

5. Discussion of the Results

To observe the quantitative effects of the spin-parameter m, particle fluid size N and the stenosis shape n, computer codes are developed for the numerical evaluations of the analytic results obtained for $\bar{\lambda}$, $\bar{\tau}_{yx}$ and $\bar{\tau}_s$ (equations (34)-(36)) for parameters values $\phi = 0$; $b = 1; L = 1, 2, 10$; $m = 0.001, 10, 100$; $N = 0, 0.1, 0.2, 0.3, 0.4, 0.5, 0.6, 0.7, 0.8$; $n = 2, 6, 11$, see [9].

In Figure 2 - Figure 5 we observe that the resistance to flow, $\bar{\lambda}$, increases with the coupling number N, and the stenosis size δ^*, while it decreases with the micropolar parameter m, stenosis length, L, and the shape parameter n and attains its maximal in the symmetric stenosis case, i.e. $n = 2$.

In Figure 6 - Figure 7 we notice that the wall shear stress distribution $\bar{\tau}_{yx}$ increases in the converging zone as the shape parameter, n, increases while it decreases in the diverging zone in a similar situation. For any given stenosis shape, the wall shear stress, $\bar{\tau}_{yx}$, steeply decreases in the upstream from its approached value (i.e, at $x = 0$) to the peak value at the throat ($\bar{\tau}_{yx}$=$\bar{\tau}_s$), then increases in the downstream of the throat and assumes its approached magnitude at the end point of the constriction profile (i.e, at $x = 1$). The rate of decreases (with respect to the axial distance) of $\bar{\tau}_{yx}$ in the upstream of the throat decreases with the increasing values of n, whereas the rate of increases of the same in the downstream of the throat increases with n.

The wall shear stress distribution $\bar{\tau}_{yx}$ and its value at the throat, $\bar{\tau}_s$, possess an inverse variations to the flow resistance, $\bar{\lambda}$, with respect to the coupling parameter N and the micropolar parameter m. $\bar{\tau}_s$ is independent of the shape and thus assumes the same magnitude for any value of n, see Figure 6 - Figure 8.

In Figure 9 - Figure 10 we study the variation of resistance to flow, $\bar{\lambda}$, with the coupling parameter N and the micropolar parameter m. In Figure 9 We observe that resistance to flow, $\bar{\lambda}$, increases with increasing the stenosis size, δ^*, and the coupling parameter, N, for any value of the micropolar parameter m. Form Figure 10 we can see that, the resistance to flow, $\bar{\lambda}$, decreases rapidly for small values of m and then take a constant value as m increases.

Finally, Figure 11 - Figure 12 show the effect of N and m on the velocity profile of the fluid u where as, N, increases (the particle size increases) the horizontal velocity u decreases and as m increases (micropolar spin parameter increases) the horizontal velocity u increases.

References

[1] S. Chakravarty, P.K. Mandal, Two-dimentional blood flow through tapered arteries under stenotic conditions, *Int. J. Non-Linear Mech.*, **35** (2000), 779-793.

[2] M. El-Shahed, Pulsatile flow of blood through a stenosed porous medium under periodic body acceleration, *Appl. Math. Comp.*, **138** (2003), 479-488.

[3] A.C. Eringen, Theory of micropolar fluid, *J. Math. Mech.*, **16** (1966).

[4] H. Jung, J.W. Choi, C.G. Park, Asymmetric flows of non-Newtonian fluids in symmetric stenosed artery, *K-A. Rheology J.*, **16** (2004), 101-108.

[5] G.T. Liu, X.J. Wang, B.Q. Ai, L.G. Liu, Numerical study of pulsating flow through a tapered artery with stenosis, *Chin. J. Phys.*, **42** (2004), 401-409.

[6] R.N. Pralhad, D.H. Schulz, Modeling of arterial stenosis and its applications to blood diseases, *Math. Bioscience*, **190** (2004), 203-220.

[7] L.M. Srivistava, Flow of couple stress fluid through stenotic blood vessels, *J. Biomech.*, **18** (1985), 479-485.

[8] V.P. Srivastava, Arterial blood flow through a nonsymmetrical stenosis with applications, *Jpn. J. Appl. Phys.*, **34** (1995), 6539-3545.

[9] D. Srinivasacharya, M. Mishra, A.R. Rao, Peristaltic pumping of a micropolar fluid in a tube, *Acta Mech.*, **161** (2003), 165-178.

[10] V.P. Srivastava, M.Saxena, Suspension model for blood flow through stenotic arteries with a cell-free plasma layer, *Math Bioscience*, **139** (1997), 79-102.

[11] D.F. Young, Effect of a time dependent stenosis of flow through a tube, *J. Eng. Ind.*, **90** (1968), 248-254.